Carbohydrate Polymers 113 (2014) 561–568

Contents lists available at ScienceDirect

Carbohydrate Polymers

journal homepage: www.elsevier.com/locate/carbpol

Electrospinning an essential oil: Cinnamaldehyde enhances the antimicrobial efficacy of chitosan/poly(ethylene oxide) nanofibers

Katrina A. Rieger, Jessica D. Schiffman*

Department of Chemical Engineering, University of Massachusetts Amherst, N533 Life Sciences Laboratories, 240 Thatcher Road, MA 01003-930, USA

ARTICLE INFO

Article history:
Received 5 May 2014
Received in revised form 6 June 2014
Accepted 12 June 2014
Available online 31 July 2014

Keywords:
Antibacterial
Chitosan
Cinnamaldehyde
Electrospin
Nanofiber
Oil-in-water

ABSTRACT

Due to the persistent spread of antibiotic resistance, commercial antibiotic treatments are proving ineffective. Cinnamaldehyde (CA), a volatile essential oil, eradicates pathogens non-specifically. However, the ability to incorporate essential oils into nanofiber mats has not yet been demonstrated, and, only six studies have electrospun two immiscible phases. Here, CA (0.5 and 5.0%) was incorporated into chitosan/poly(ethylene oxide) (PEO) solutions that were successfully electrospun into mats with ~50 nm fiber diameters. Solid-state NMR results corroborated with release studies wherein the 5.0% CA mats released a statistically higher amount of CA-liquid (545% more) and CA-vapor (279% more) than the 0.5% CA mats. In time dependent cytotoxicity studies, the intrinsic antibacterial activity of chitosan along with the quick release of CA enabled high inactivation rates against *Escherichia coli* and *Pseudomonas aeruginosa*. For the first time we have demonstrated chitosan/CA/PEO nanofiber mats can serve as CA delivery vehicles that potentially eradicate pseudomonas infections.

© 2014 Elsevier Ltd. All rights reserved.

1. Introduction

Annually in the United States, 1.7 million patients are inflicted with bacterial infections, and of those, ~99,000 result in death (Kleven, Edwards, Richards, & Horan, 2007). Approximately half of these mortalities have been linked to *Pseudomonas aeruginosa* (*P. aeruginosa*), the leading Gram-negative opportunistic human pathogen (Fick, 1993; Page & Heim, 2009). Notably, once planktonic *P. aeruginosa* develop into a microbial community called a biofilm, they become 1000 times more resistant to antibiotics than when the bacteria were in the planktonic state (de Kievit, 2009; Donlan, 2002; Rasmussen & Givskov, 2006). Thus, new materials that can delay the onset of *P. aeruginosa* biofilm formation, while avoiding the spread of resistance genes, are in high demand.

For centuries, plant-derived essential oils have been used to fight bacterial infections (Bakkali, Averbeck, Averbeck, & Idaomar, 2008). Due to their complex antimicrobial mechanisms, the development of resistance by bacteria to these volatile extracts has not yet been reported. Numerous review articles (Burt, 2004; Hammer, Carson, & Riley, 1999; Pattnaik, Suramanyam, Bapaji, & Kole, 1997) have summarized that the essential oils contain small, hydrophobic terpenoid or phenolic compounds that can easily permeate the cell membrane leading to a depletion of the proton gradient and a subsequent disruption of adenosine triphosphate (ATP) synthesis or cell lysis (Burt, 2004). Cinnamaldehyde (CA) is a well-studied essential oil derived from cinnamon bark, which is effective against *P. aeruginosa* at a minimum inhibitory concentration (MIC) of 300 μg/mL (Ooi et al., 2006). Additionally, sublethal concentrations of CA act as a quorum sensing inhibitor, interfering with the autoinducer-2 (AI-2) system present in *P. aeruginosa* biofilms (Jia, Xue, Duan, & Shao, 2011; Niu, Afre, & Gilbert, 2006; Rasmussen & Givskov, 2006). Despite the historic use of essential oils as antibacterial agents, previous studies are limited in scope. Essential oils have been delivered via carrier-solutions, polymer derivatives, or encapsulated in solid particles/films (Badawy & Rabea, 2013; Dorman & Deans, 2000; Hammer et al., 1999; Kavanaugh & Ribbeck, 2012; Ojagh, Rezaei, Razavi, & Hosseini, 2010; Zodrow, Schiffman, & Elimelech, 2012); however, for proper wound healing, a porous and permeable scaffold would be optimal.

Electrospun nanofiber mats are flexible, highly porous, permeable materials that provide a high surface-to-volume ratio ideal for wound dressings (Engel, Schiffman, Goddard, & Rotello, 2012; Rieger, Birch, & Schiffman, 2013; Zhang, Lim, Ramakrishna, & Huang, 2005). The well-established technique of electrospinning has been utilized to produce non-woven mats from over 100 different synthetic and natural polymer solutions (Frey, 2008; Liu et al., 2010; Pakravan, Heuzey, & Ajji, 2011; Rutledge & Fridrikh, 2007; Schiffman & Schauer, 2007a, 2008; Teo & Ramakrishna, 2006). Despite recent progress in electrospinning, parameters that govern the ability to spin an oil or another water-immiscible phase

* Corresponding author. Tel.: +1 413 545 6143; fax: +1 413 545 1647.
E-mail address: schiffman@ecs.umass.edu (J.D. Schiffman).

http://dx.doi.org/10.1016/j.carbpol.2014.06.075
0144-8617/© 2014 Elsevier Ltd. All rights reserved.

is limited. Previously, only six studies have spun two immiscible phases by utilizing a surfactant to stabilize drops of one phase against coalescence (Angeles, Cheng, & Velankar, 2008; Briggs & Arinzeh, 2014; Li, Ko, & Hamad, 2013; Sanders, Kloefkorn, Bowlin, Simpson, & Wnek, 2003; Xu et al., 2005, 2006). Five of those manuscripts demonstrated spinning a water-in-oil emulsion featuring a water soluble agent or a hydrophilic polymer inside a hydrophobic/amphiphilic polymer (Briggs & Arinzeh, 2014; Li et al., 2013; Sanders et al., 2003; Xu et al., 2005, 2006). One study (Angeles et al., 2008) demonstrated the ability to electrospin an oil-in-water emulsion, which featured an aqueous solution of poly(ethylene oxide) (PEO) as the continuous phase and mineral oil (a non-volatile oil) as the drop phase.

In this work, we aim to avoid the use of potentially toxic surfactants (Cserháti, Forgács, & Oros, 2002) by demonstrating that the essential oil, CA, can be electrospun using chitosan, a "green" hydrophilic polymer. Chitosan, the cationic (1-4)-2-amino-2-deoxy-β-D-glucan partly acetylated to ~0.25, is industrially produced from marine chitin (Aranaz et al., 2009; Honarkar & Barikani, 2009; Krajewska, 2005; Muzzarelli, 1977, 2012; Muzzarelli et al., 2012; Rinaudo, 2006). The two blocks of chitosan allow the biopolymer to act as a stabilizer (Iamsamai, Hannongbua, Ruktanonchai, Soottitantawat, & Dubas, 2010; Rodraguez, 2002; Schulz, Rodríguez, Del Blanco, Pistonesi, & Agulló, 1998; Yan, Poon, Chan-Park, Chen, & Zhang, 2008). Additionally, the availability of the positive charge on the C-2 of the glucosamine monomer enables its antibacterial activity (An, Zhang, Zhang, Zhao, & Yuan, 2009; Badawy & Rabea, 2011; Krajewska, Wydro, & Jańczyk, 2011; Krajewska, Wydro, & Kyzioł, 2013a; Rabea, Badawy, Stevens, Smagghe, & Steurbaut, 2003) and previously, chitosan/PEO nanofiber mats have demonstrated a strong antibacterial activity against *Escherichia coli* (An et al., 2009). Here, we explored the engineered incorporation, delivery, and cytotoxicity of electrospun nanofiber mats featuring an essential oil.

2. Materials and methods

2.1. Materials and chemicals

All compounds were used as received. Chitosan (product no. 448869, Mw = 460,000 Da), poly(ethylene oxide) (PEO, Mw = 600,000 Da), cinnamaldehyde (CA, ≥93%, FG, Mw = 132.16 Da), analytical reagent grade acetic acid (AA), sodium chloride (NaCl), glutaraldehyde (GA, 50 wt% aqueous solution), deuterium oxide, and acetic acid-d4 (AA-d4) were obtained from Sigma-Aldrich (St. Louis, MO). Sodium hydroxide (NaOH) was obtained from Fisher Scientific (Fair Lawn, NJ). Difco Luria-Bertani (LB) broth was purchased from BD Life Sciences (Franklin Lakes, NJ). Propidium iodide (PI) and 4′,6-diamidino-2-phenylindole (DAPI) were purchased from Invitrogen (Carlsbad, CA). Deionized (DI) water was obtained from a Barnstead Nanopure Infinity water purification system (Thermo Fisher Scientific, Waltham, WA).

2.2. Chitosan/CA Schiff base quantification

Proton nuclear magnetic resonance (^{1}H NMR, Bruker Avance 400) along with SpinWorks3, an NMR analysis software, were employed to quantitatively determine the degree of acetylation (DA) and degree of substitution (DS) of the chitosan. Chitosan (2.5 w/v%, 15 mg) was dissolved in AA-d4 (600 μL) using an Arma-Rotator A-1 (Bethesda, MA) to determine the DA. CA was added (0, 0.5, and 5.0 v/v% CA) to 2.5 w/v% chitosan dissolved in 0.5 M AA-d4 (600 μL) to determine the DS. DA values were determined by taking the relative integrals of 1.7–2.4 ppm over 2.7–4.4 ppm, (Fernandez-Megia, Novoa-Carballal, Quiñoá, & Riguera, 2005; Hirai, Odani, & Nakajima, 1991; Varum, Antohonsen, Grasdalen, & Smidsrød, 1991) as outlined by Fernandez-Megia et al. (2005).

2.3. Chitosan/CA/PEO nanofiber mat fabrication

A 1:1 ratio of chitosan to PEO (0.5 g:0.5 g) in 0.5 M AA (20 mL) corresponding to a 5.0 w/v% solution was mixed for 24 h at 20 rpm using an Arma-Rotator A-1 (Bethesda, MA). Various amounts of CA (0 mL, 0.1 mL, and 1.0 mL corresponding to 0, 0.5, and 5.0 v/v%, respectively) were added to the solution and mixed for an additional 24 h at which point, the solution changed from transparent to white. Throughout the mixing process, the solution had a pH value of 4.

Each chitosan/CA(0, 0.5, or 5.0%)/PEO solution was loaded into a 5 mL Luer-Lock tip syringe capped with a Precision Glide 18 gauge needle (Becton, Dickinson & Co. Franklin Lakes, NJ), which was secured to a PHD Ultra syringe pump (Harvard Apparatus, Plymouth Meeting, PA). Alligator clips were used to connect the positive anode of a high-voltage supply (Gamma High Voltage Research Inc., Ormond Beach, FL) to the needle and the negative anode to a copper plate wrapped in aluminium foil. A constant feed rate of 60 μL/min, an applied voltage of 25 kV, and a separation distance of 120, 160, and 140 mm were used to electrospin chitosan/CA(0, 0.5, and 5.0%)/PEO solutions, respectively. The assembled electrospinning apparatus was housed in an environmental chamber (CleaTech, Santa Ana, CA) with a desiccant unit (Drierite, Xenia, OH) to maintain a temperature of 22 ± 1 °C and a relative humidity of 24–28%. All nanofiber mats used in release and bacterial studies were spun for 1 h. All as-spun mats were crosslinked using GA vapor as previously described (Schiffman & Schauer, 2007b). Briefly, mats were placed in a vapor chamber (122 mm × 98 mm × 78 mm, Biohit Inc, Neptune, NJ) containing 1.0 mL of GA liquid, 50 wt% aqueous solution. At room temperature (23 °C), the GA liquid vaporized and was allowed to crosslink the fibers for 4 h. This ensured the chemical stability of the nanofiber mats for release studies and antibacterial evaluation.

2.4. Chitosan/CA/PEO nanofiber mat characterization

Micrographs were acquired using a FEI-Magellan 400 scanning electron microscope (SEM). A Gatan high resolution ion beam coater model 681 was used to sputter coat samples for 4 min with platinum. Fiber diameter distribution was determined by Image J 1.45 software (National Institutes of Health, Bethesda, MD) by measuring 50 random fibers from 5 micrographs. By following the parameters suggested by Guinesi and Cavalheiro (2006b) and Jatunov, Franconetti, Gomez-Guillen, and Cabrera-Escribano (2012) carbon-13 NMR (^{13}C NMR, DSX300) and SpinWorks3 were employed to confirm the presence of chitosan, PEO, and CA within the as-spun mats. Approximately 50 mg of chitosan/CA(0, 0.5, and 5.0%)/PEO nanofiber mat, as well as a 100 mg powder sample of chitosan:PEO (1:1) were analyzed.

2.5. Liquid and vapor state release of CA from chitosan/CA/PEO nanofiber mats

The release characteristics of CA as a liquid (CA-liquid) and as a vapor (CA-vapor) from the nanofiber mats were quantified at times relevant to antibacterial activity experiments. Consistent chitosan/CA(0, 0.5, and 5.0%)/PEO nanofiber mats (10 mm × 20 mm) were placed into 1.5 mL centrifuge tubes containing 1.0 mL of an isotonic solution (0.9% NaCl, pH 5.7) with virtually no headspace. The samples were maintained at 37 °C and shaken at 100 rpm. As a function of time, all of the isotonic solution (1.0 mL) was removed via needle/syringe and placed in a cuvette for analysis. After testing, the 1.0 mL was returned to the vial until the next time point.

The amount of CA-liquid present in the isotonic solution was determined using UV–vis spectroscopy (UV–vis, Agilent Diode Array) at an absorbance of 293 nm (Talrose et al., 2007; Yang et al., 2012). The solution was placed back into the sample to maintain the same gradient flux.

As a function of time, quantification of the CA-vapor released from the mat into the headspace of the vial was performed using gas chromatography, GC (Agilent/HP 6890 equipped with a flame ionization detector) (Friedman, Kozukue, & Harden, 2000). Nanofiber mats (10 mm × 20 mm) were placed in 10 mL of isotonic solution with 10 mL of headspace in the vial for the CA-vapor to accumulate. The sealed vials were kept at 37 °C and shaken at 100 rpm. Manual samples containing 1 mL of gas were injected into the GC at 30, 90, and 180 min intervals. Standard calibration curves were determined for both UV–vis and GC to quantify the amount of CA in each sample. Chitosan/CA(0%)/PEO mats were used as controls.

2.6. Evaluation of antibacterial activity of electrospun chitosan/CA/PEO nanofiber mats

The model organisms were *Escherichia coli* S20918 (*E. coli*) and *P. aeruginosa* S20930 (*P. aeruginosa*), purchased from Thermo Fisher Scientific, Waltham, WA. The bacteria were grown in LB at 37 °C and harvested at a concentration of 10^8 cells/mL. To remove residual macromolecules and other growth medium constituents, cells were washed twice and then resuspended in an isotonic solution (0.9% NaCl, pH 5.7). This isotonic solution was used for *E. coli* and *P. aeruginosa* loss of viability studies.

The viability loss of *E. coli* in contact with chitosan/CA(0, 0.5, and 5.0%)/PEO nanofiber mats was assayed according to a modified ASTM shake flask method (American Society for Testing and Materials (ASTM), 2004). In parallel to each experiment (i) a blank control (no nanofiber mat) and (ii) an MIC control of CA for *E. coli* (3 mM CA in solution) were employed. (Zodrow et al., 2012) Electrospun mats (10 mm × 20 mm) were placed into culture tubes (16 mm × 125 mm) along with 4 mL suspensions of *E. coli* or *P. aeruginosa* (5×10^6 cells/mL) in an isotonic solution (0.9% NaCl, pH 5.7). The suspensions were shaken at 200 rpm in an orbital shaker maintained at 37 °C. At 30, 90, and 180 min, 100 μL were pipetted out from the tubes and serial dilutions were plated onto LB plates using the spread plate method (American Society for Testing and Materials (ASTM), 2004; Chen, Bromberg, Hatton, & Rutledge, 2008; Fu, Ji, Yuan, & Shen, 2005). After 24 h incubation on agar plates, the number of viable bacteria were counted then multiplied by the dilution factor and expressed as the mean colony forming unit (CFU) per mL. The percent reduction of bacteria resulting from contact with the nanofiber mats was determined using Eq. (1), where A represents the mean $\log_{10}$ density of bacteria for the flask containing the treated substrate after the specified contact time and B represents the untreated substrate after the specified contact time.

$$\text{Reduction of bacteria } (\%) = \frac{B - A}{B} \times 100 \quad (1)$$

Viability loss of *P. aeruginosa* in contact with chitosan/CA(0, 0.5, and 5.0%)/PEO nanofiber mats was determined using a previously described fluorescence assay (Schiffman, Wang, Giannelis, & Elimelech, 2011). Electrospun mats (20 mm × 10 mm) were placed at the bottom of 35 mm × 10 mm petri dishes (Becton, Dickinson & Co., Franklin Lakes, NJ) to which the cells (10^7 cells/mL), resuspended in an isotonic solution(0.9% NaCl, pH 5.7), were added and diluted by a factor of 2. The cells were incubated at 37 °C for various times (30, 90, and 180 min), then stained in the dark with PI (excitation/emission at 535 nm/617 nm) for 15 min, after which they were counter-stained with DAPI (excitation/emission at 358 nm/461 nm). Fluorescence images were acquired to detect the cells utilizing an epifluorescence microscope (Olympus) with a Chroma cube filter. At various locations of each specimen, five representative images were taken at 20× magnification. Dead cells and the total number of cells were determined by direct cell counting. Loss of viability was taken as the ratio of the number of cells stained with PI divided by the number of cells stained with DAPI plus PI. In parallel to each experiment (i) a blank control (no nanofiber mat) and (ii) an MIC control of CA for *P. aeruginosa* (3 mM CA in solution) were employed (Zodrow et al., 2012). All reported statistical differences were determined using an unpaired *t*-test with values of $p \leq 0.05$ considered to be statistically significant.

3. Results and discussion

3.1. Chitosan/CA/PEO precursor solution characteristics

Using ^{1}H NMR, the degree of *N*-acetylation (DA) of chitosan was determined to be 13% (Fernandez-Megia et al., 2005; Hirai et al., 1991; Varum et al., 1991). We blended our chitosan/PEO solutions in aqueous acetic acid solutions maintained at a pH value of 4, which is known to enhance Schiff base reactions (Cordes & Jencks, 1962; Pine, Hendrickson, Cram, & Hammono, 1980). The degree of substitution (DS)—the ratio of amines reacted with CA over the total amount of amines (Guinesi & Cavalheiro, 2006a) was characterized using the ^{1}H NMR peaks at 9.0 ppm and 9.5 ppm (Ganjian, Baumgarten, & Valenzuela, 1992), which correspond to the presence of unreacted and reacted CA, respectively (Fig. 1). DS values were calculated from the ratio of the integrated resonances of reacted CA (9.25–9.6 ppm) over glucosamine residues on

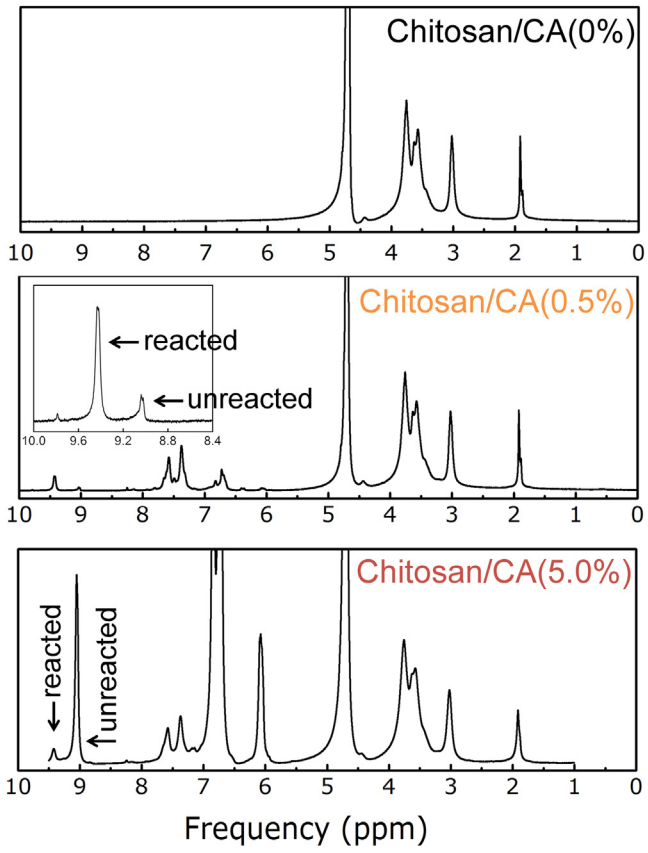

Fig. 1. (Top to bottom) The ^{1}H NMR spectra of chitosan solutions mixed with 0, 0.5, and 5.0% CA. Quantitatively, the chitosan/CA(0.5 and 5.0%) solutions have the same amount of Schiff base reacted CA. However, the chitosan/CA(5.0%) solution contains a statistically higher amount of unreacted CA than the 0.5% CA solution. An enlarged inset plot is provided to clarify the reacted and unreacted CA peaks in the chitosan/CA(0.5%) spectra. PEO was not included in the NMR solutions.

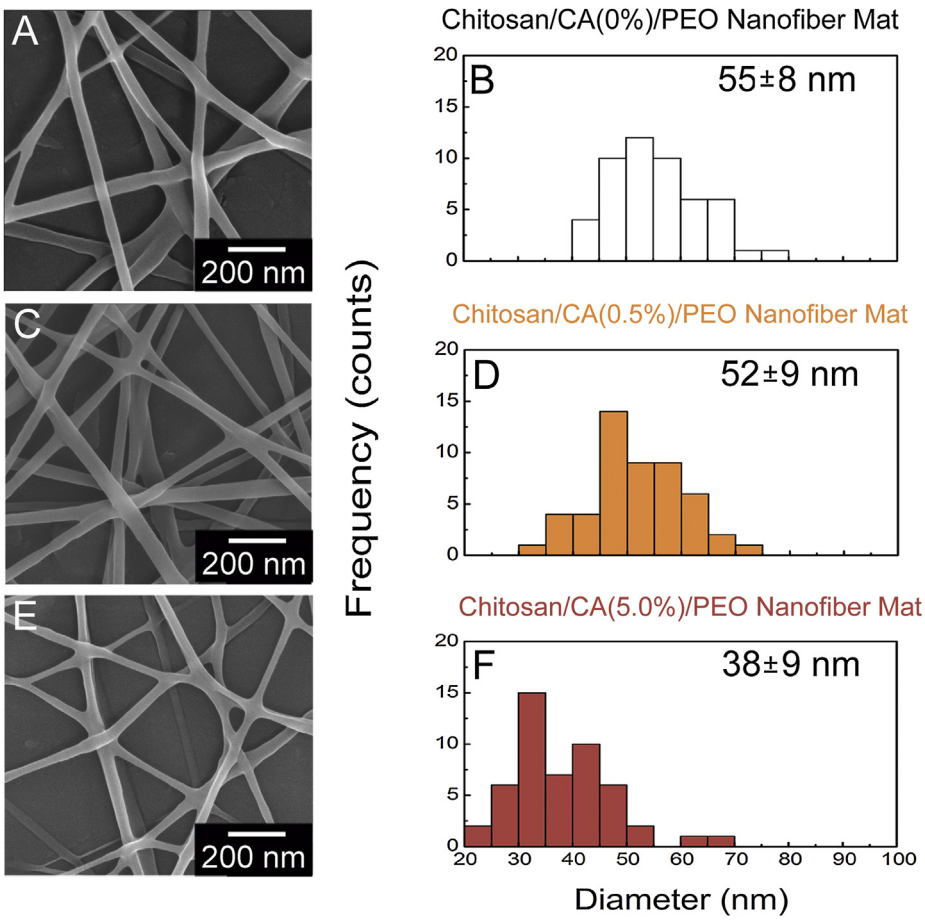

Fig. 2. SEM micrographs ((A), (C), and (E)) displaying the morphology of chitosan/CA(0, 0.5, and 5.0%)/PEO nanofiber mats, respectively. Fiber diameter distribution ((B), (D), and (F)) is displayed along with the average fiber diameter and standard deviation ($n = 50$). The average fiber diameter of the chitosan/CA(0, 0.5, and 5.0%)/PEO mats are statistically equivalent based on an unpaired student t-test.

chitosan (2.7–4.4 ppm). It was determined that chitosan solutions mixed with 0.5 and 5.0% CA yielded comparable DS values, 15% and 16%, respectively. While our initial chitosan had 87% free amines, after mixing the chitosan/CA(0.5 and 5.0%) derivatives had ~70% free amines remaining. Importantly, the ^{1}H NMR spectra revealed that unreacted CA is also present indicating that chitosan is physically entrapping the volatile oil. The chitosan/CA(0.5%) derivative contains 28% unreacted CA, while the chitosan/CA(5.0%) derivative contains a statistically higher, 89% unreacted CA.

3.2. Chitosan/CA/PEO nanofiber mat physical characteristics

Chitosan/CA(0%)/PEO nanofiber mats were successfully electrospun from a 5.0 w/v% solution containing an equal mass ratio of the two polymers. As displayed on Fig. 2A, the chitosan/CA(0%)/PEO nanofiber mats were composed of continuous, fine, cylindrical fibers, consistent with the morphology previously reported (An et al., 2009; Pakravan et al., 2011). Nanofiber mats were also effectively electrospun from solutions containing the two different CA loadings, chitosan/CA(0.5 and 5.0%)/PEO with the polymers at a 1:1 ratio (Fig. 2C and E).

Average fiber diameters ($n = 50$) for the electrospun chitosan/CA(0, 0.5, and 5.0%)/PEO nanofiber mats are displayed in Fig. 2. The chitosan/CA(0, 0.5, and 5.0%)/PEO nanofiber mats had average fiber diameters of 55 ± 8 nm, 52 ± 9 nm, and 38 ± 9 nm, respectively, which was similar to the chitosan/PEO nanofiber mats previously spun in literature. An unpaired t-test between the chitosan/CA(0%)/PEO and the chitosan/CA(0.5 and 5.0%)/PEO mats determined that the variation in fiber diameter was not statistically significant. Simply put, on average, by slight modification to our electrospinning parameters, we were able to produce fiber diameters that did not change due to the presence of CA.

It is important to note that attempts to electrospin solutions containing only PEO and CA (no chitosan) phase separated: a homogeneous solution appropriate for electrospinning could not be obtained. This suggests that in our system the chitosan is (i) chemically reacting with CA (Cordes & Jencks, 1962; Pine et al., 1980) as observed in ^{1}H NMR and (ii) acts as a stabilizer (Iamsamai et al., 2010; Rodraguez, 2002; Schulz et al., 1998; Yan et al., 2008) to physically incorporate the CA into the precurser solution. In Section 3.3, we will provide confirmation that the CA remains in the nanofibers post-electrospinning.

In order for release studies and antibacterial testing to be conducted, increased chemical stability of chitosan/CA(0, 0.5, and 5.0%)/PEO nanofiber mats was achieved using a slightly modified glutaraldehyde crosslinking protocol (Schiffman & Schauer, 2007b). The carbonyl groups of glutaraldehyde can form a Schiff base reaction with the free amino groups at the C-2 position of chitosan and an acetalization reaction with the hydroxyl groups at the C-6 position of chitosan(Schiffman & Schauer, 2007b). Based on our ^{1}H NMR results, all chitosan/CA(0, 0.5, and 5.0%) derivative solutions have an abundant quantity of free amine groups ranging from 84–71% for both crosslinking and antibacterial activity. After crosslinking for 4 h, the average fiber diameter for the crosslinked chitosan/CA(0, 0.5, and 5.0%)/PEO fiber mats were statistically the same as the as-spun chitosan/CA(0, 0.5, and 5.0%)/PEO mats: 53 ± 8 nm for 0% CA,

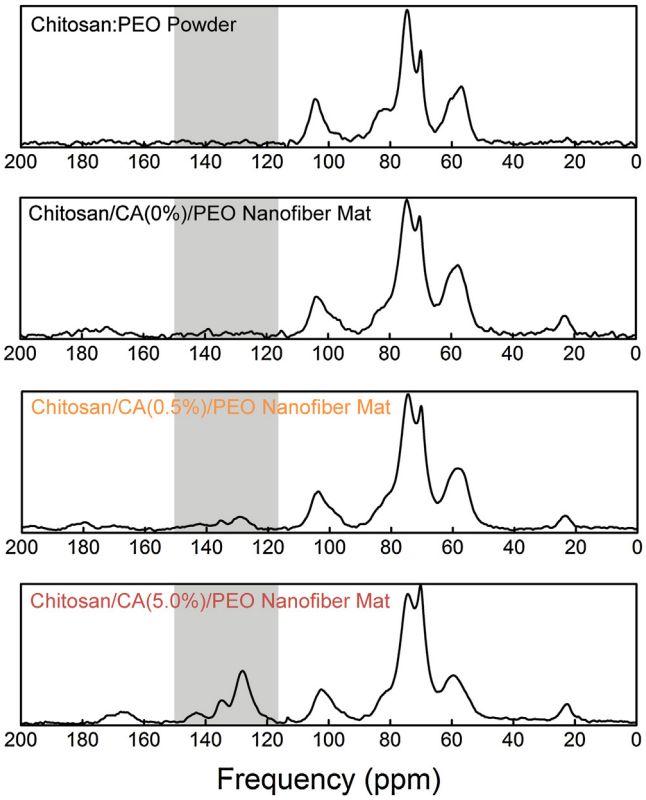

Fig. 3. Displayed is the solid state ^{13}C NMR spectra of (top-to-bottom) chitosan:PEO powder (control) and electrospun chitosan/CA(0, 0.5, and 5.0%) nanofiber mats. Peaks between 120 and 150, as well as at 170 ppm confirm the presence of CA in the chitosan/CA(0.5 and 5.0%)/PEO nanofiber mats.

56 ± 11 nm for 0.5%, and 41 ± 6 nm for 5.0% CA. SEM micrographs of the crosslinked nanofiber mats 72 h post-submersion in acidic, neutral, and basic solutions (not shown) confirmed that the nanofibrous morphology of the mats was retained. Additionally, after the release studies and antibacterial evaluation described below, acquired SEM micrographs confirmed that the nanofiber morphology remained intact (not shown).

3.3. Chitosan/CA/PEO nanofiber mat chemical characteristics

To qualitatively ensure that attached and unattached CA were present in the as-spun nanofiber mats, solid state ^{13}C NMR was conducted, Fig. 3. The spectra suggests that due to the presence of CA (i) the height of the aromatic peak (Jatunov et al., 2012) is greater for nanofibers spun with 5.0% CA than those spun from 0.5% CA, while (ii) the imine peak at 170 ppm (Jatunov et al., 2012) is smaller than that observed for the aromatic peaks. This corroborates the solution NMR data: the majority of CA within the nanofiber mat is physically entrapped, unreacted CA. These peaks are absent from the control spectra acquired on chitosan/CA(0%)/PEO nanofiber mats and chitosan:PEO powder. "Control" chitosan/CA/PEO nanofiber mats electrospun from the same solvent system with only unreacted CA could not be obtained as the Schiff base is pH dependent. Further increasing the pH (beyond where Schiff bases are encouraged) resulted in chitosan that was not fully dissolved.

3.4. Release characteristics of chitosan/CA/PEO nanofiber mats

The release characteristics of CA-liquid and CA-vapor from the nanofiber mats were quantified using UV–vis, Fig. 4A and B, respectively. Experiments were conducted at physiological temperature (37 °C) at times relevant to antibacterial activity tests. Preliminary experiments determined that using small, 1.5 mL vials, minimized the vapor space and kept the CA-liquid highly concentrated, thus enabling the acquisition of the most accurate UV–vis data. Fig. 4A displays that as a function of time, the release of CA continues to gradually increase from the chitosan/CA(0.5 and 5.0%)/PEO nanofiber mats. After 15 min, the chitosan/CA(0.5 and 5.0%)/PEO nanofiber mats demonstrated an initial CA-liquid release of $2.0 \times 10^{-3} \pm 3 \times 10^{-4}$ μg and $1.9 \times 10^{-3} \pm 1 \times 10^{-4}$ μg, respectively. At longer times (90 and 180 min), the amount of CA released started to level off indicating that equilibrium has been reached (Peppas, Bures, Leobandung, & Ichikawa, 2000; Siepmann & Peppas, 2011). Specifically, CA-liquid release reached quantities of $2.7 \times 10^{-3} \pm 9 \times 10^{-4}$ μg and $1.5 \times 10^{-2} \pm 4 \times 10^{-3}$ μg after 180 min for the chitosan/CA(0.5 and 5.0%) nanofiber mats, respectively. Between 30 and 180 min, the cumulative amount of CA-liquid released from the chitosan/CA(5.0%)/PEO nanofiber mats is statistically higher than the CA-liquid released from the chitosan/CA(0.5%)/PEO nanofiber mats. Overall, 545% more CA was released from the mats spun with a higher CA concentration.

In addition to the CA-liquid release, due to the volatility of the essential oil, it is likely that a significant amount of CA-vapor will occupy the surrounding air space (Edris, 2007). GC was employed to quantify the CA-vapor released into the vial headspace (Fig. 4B). In contrast to the UV–vis, larger vials (20 mL) were used for accurate GC data to gain more air space to increase the sampling volume. From samples acquired after 30 min it was determined that 0.6 ± 0.1 μg of CA-vapor was released from the chitosan/CA(0.5%)/PEO nanofiber mats and that a statistically equivalent amount of CA-vapor, 0.9 ± 0.3 μg, was released from the chitosan/CA(5.0%)/PEO nanofiber mats. At 90 min, the CA-vapor released from chitosan/CA(0.5%)/PEO (0.6 ± 0.1 μg) and from the chitosan/CA(5.0%)/PEO (0.7 ± 0.2 μg) nanofiber mats were statistically equivalent. After 180 min, the quantity of CA-vapor released from the chitosan/CA(5.0%)/PEO nanofiber mats was statistically higher than the quantity released from the chitosan/CA(0.5%)/PEO mats, 0.7 ± 0.1 μg versus 0.3 ± 0.1 μg. Statistically, the same quantity of CA occupies the vapor headspace at all three time points investigated for each chitosan/CA/PEO nanofiber mats system (0.5 and 5.0%) thus indicating that the CA-vapor releases quickly. The chitosan/CA(5.0%)/PEO nanofiber mats released 279% more CA-vapor after 180 min than chitosan/CA(0.5%)/PEO nanofiber mats. The use of different collection set-ups for liquid and vapor release means that we cannot plot a reliable total release curve. However, we can state that more vapor-CA is released than liquid-CA, which further emphasizes the importance of characterizing the vapor phase release even though most previous studies only quantify release into the liquid phase (Yang et al., 2012).

Literature reports three potential mechanisms for release: swelling-controlled, diffusion-controlled, and reaction-controlled, all of which are highly pH dependent (Peppas et al., 2000; Siepmann & Peppas, 2011). The governing mechanism of release depends on whether the CA is attached or unattached to the chitosan. Solid-state ^{13}C NMR informs that the majority of CA in our chitosan/CA(0.5 and 5.0%)/PEO nanofiber mats is physically incorporated and therefore swelling controlled. Unreacted CA is likely to be released by the swelling of the chitosan and PEO once the nanofiber mats are submerged in the isotonic solution. Initial release testing at a range of pHs indicated that minimal release of CA occurred in basic conditions (pH of 8 or greater) where the nanofibers would have minimal swelling (not shown). Based on previous literature, we hypothesize that the CA diffuses through the mixed polymer network following Fickian diffusion (Verreck et al., 2003). While accurately modeling the diffusion behavior is beyond the scope of this manuscript, it remains a goal for our future work.

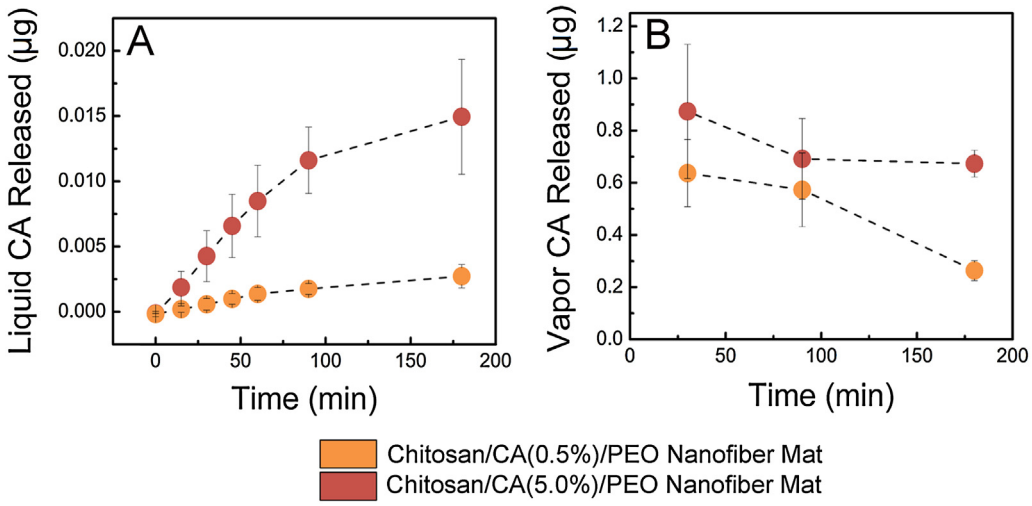

Fig. 4. (A) The quantity of CA-liquid released from chitosan/CA(0.5 and 5.0%)/PEO nanofiber mats was determined through UV–vis spectroscopy. (B) Using gas chromatography GC, the amount of CA-vapor released from the chitosan/CA(0.5 and 5.0%)/PEO nanofiber mats was determined. Error bars indicate one standard deviation.

3.5. Antibacterial activity of chitosan/CA/PEO nanofiber mats against E. coli

After only 30 min of nanofiber-bacteria contact, a high level of inactivation against *E. coli* is achieved, Fig. 5. Statistically, all three of our nanofiber mats demonstrated a complete inactivation at all incubation times evaluated (30, 90, and 180 min). Observed inactivation values for mats incubated for 180 min were at the limit of the accuracy or range of the bacterial viability assay. As displayed on Fig. 5, any value greater than 99% must be considered only as >99% (Schiffman et al., 2011). These results are consistent with previous research (An et al., 2009), where nanofiber mats electrospun from a 5.0 wt% solution of chitosan/PEO (1/1) exhibited increased cytotoxicity against *E. coli* for 4 h. A low, statistically smaller loss of viability occurred in the blank control experiment (no nanofiber mat or antibacterial agent present).

The MIC control (3 mM CA solution, no nanofiber mat) allows for a comparison of the effect of CA has on *E. coli* inactivation (Zodrow et al., 2012). The MIC control statistically inactivated more *E. coli* than the blank control confirming previous reports that CA displays antibacterial activity against *E. coli*. Interestingly, after 30 and 180 min, the MIC control displayed a statistically lower level of antibacterial activity than chitosan/CA(0, 0.5, and 5.0%)/PEO nanofiber mats. At 90 min, the MIC control was statistically equivalent to the chitosan/CA(0.5%)/PEO nanofiber mats. These results suggest that at shorter times, CA alone may be less effective than the nanofiber mats.

The chitosan in the chitosan/CA(0%)/PEO nanofiber mats offer positively charged free amine groups, which damages the bacterial membrane's ability to function as a barrier (Helander, Nurmiaho-Lassila, Ahvenainen, Rhoades, & Roller, 2001; Krajewska, Kyzioł, & Wydro, 2013b; Krajewska et al., 2011; Krajewska et al., 2013b; Liu, Du, Wang, & Sun, 2004). Chitosan/CA(0.5 and 5.0%)/PEO nanofiber mats offer an additional mechanism to inactivate bacteria: direct contact between microbes and the CA (Oussalah, Caillet, & Lacroix, 2006). While nanofiber mats containing attached CA offer less free amines to interact with microbes, the statistical equivalence of antibacterial efficacy achieved by all three chitosan/CA/PEO nanofiber systems confirms that by a using a combination of chitosan and CA killing mechanisms, a complete inactivation of *E. coli* can be achieved.

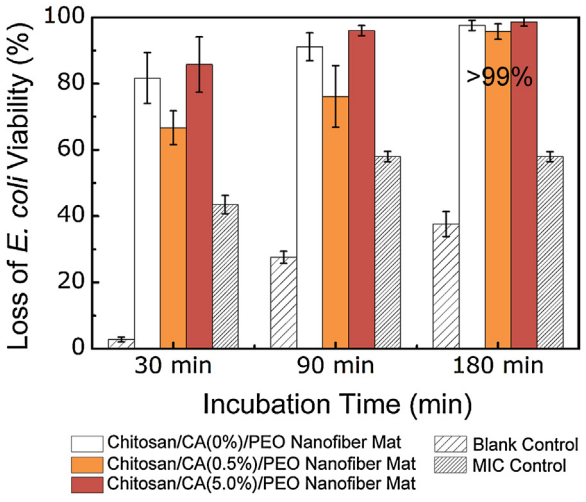

Fig. 5. A complete inactivation of *E. coli* was achieved by chitosan/CA(0, 0.5, and 5.0%)/PEO nanofiber mats at all incubation times. The MIC control (3 mM CA) was always statistically higher than the blank control (no nanofiber mat). Experiments were performed in triplicates and error bars indicate one standard error.

3.6. Antibacterial activity of chitosan/CA/PEO nanofiber mats against P. aeruginosa

The efficacy of any chitosan-based nanofiber mats against *P. aeruginosa* has not yet been reported. Notably, fewer antibiotics are effective against this strain of microbe (Page & Heim, 2009). Fig. 6 displays that after 30 min, statistically equal levels of *P. aeruginosa* inactivation were demonstrated by all three nanofiber mats. An initial efficacy of 50 ± 6% against *P. aeruginosa* was demonstrated by the chitosan/CA(0%)/PEO nanofiber mats confirming the strong intrinsic cytotoxicity of chitosan, which was statistically equivalent to the MIC control. Once 90 min of incubation was reached, the chitosan/CA(5.0%)/PEO nanofiber mats achieved a higher rate of inactivation (76 ± 8%) compared to the chitosan/CA(0 and 0.5%)/PEO nanofiber mats (48 ± 4% and 54 ± 9%). The higher antibacterial activity of chitosan/CA(5.0%)/PEO nanofiber mats is most likely due to the higher release of CA. The MIC control at 90 min inactivated *P. aeruginosa* at a statistically equivalent level as the chitosan/CA(0.5 and 5.0%)/PEO nanofiber mats, thus validating the contribution of CA to the increased antibacterial activity exhibited by the chitosan/CA(5.0%)/PEO nanofiber mats. After 180 min, chitosan/CA(0, 0.5, and 5.0%)/PEO nanofiber mats

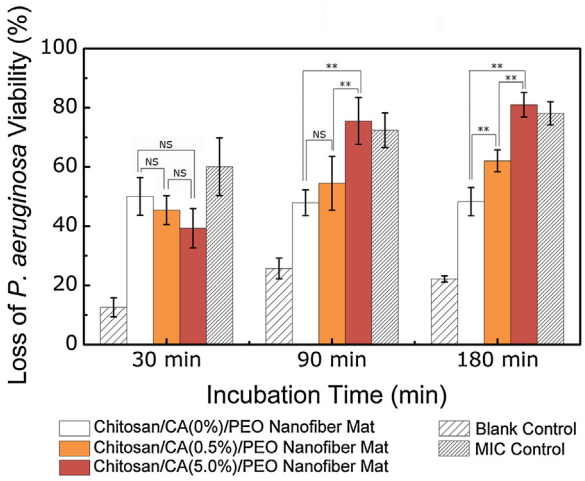

Fig. 6. The loss of *P. aeruginosa* viability as a function of incubation time for chitosan/CA(0, 0.5, and 5.0%)/PEO nanofiber mats. Also displayed is the blank control (no nanofiber mat) and an MIC control (3 mM CA). Experiments were performed in triplicate, NS denotes not significant, and error bars indicate one standard error.

exhibited statistically different rates of inactivation. Inactivation of *P. aeruginosa* increased with increasing CA content. The chitosan/CA(0, 0.5, and 5.0%)/PEO nanofiber mats inactivated 48 ± 5%, 62 ± 4%, and 81 ± 4% of *P. aeruginosa*, respectively. The MIC control (at 180 min) statistically inactivated the same level of bacteria as the chitosan/CA(5.0%)/PEO nanofiber mats. The statistically higher inactivation parallels the statistical increase in CA release (liquid and vapor) from the nanofiber mats over the 180 min (Fig. 3). At all times, the blank control exhibited a statistically lower loss of viability. While literature supports that higher concentrations of CA released as vapor should increase microbial inactivation,(López, Sanchez, Batlle, & Nerín, 2007) there is a limit to the desired CA incorporation. The amount of CA within our nanofiber mats is under the level toxic to mammalian cells yet high enough to achieve a strong level of *P. aeruginosa* inactivation.

4. Conclusion

An essential oil, CA, was successfully electrospun and delivered from chitosan/PEO nanofiber mats, without the use of a surfactant. An intrinsically antibacterial biopolymer, chitosan aided in CA incorporation while PEO allowed access to spinnable solutions at a pH value of 4. Solution and solid state NMR on precursor solutions and as-spun mats respectively determined that the attached-CA and unattached-CA were present in both. At physiological conditions, the polymer nanofiber mats released the CA-liquid and CA-vapor. Over 180 min, the quantity of CA-vapor was two orders of magnitude greater than CA-liquid with statistically higher levels of release from chitosan/CA(5.0%)/PEO nanofiber mats in both phases. Within 30 min, chitosan/CA(0%)/PEO nanofiber mats achieved a full inactivation of *E. coli*. Exploration into the cytotoxicity of the chitosan/CA(0%)/PEO nanofiber mats towards *P. aeruginosa* had not yet been demonstrated, and was determined to have a strong effect, inactivating ~50% of the microbe. The release of CA from the chitosan/CA(0.5 and 5.0%)/PEO nanofiber mats directly influenced their cytotoxicity against *P. aeruginosa*. After 180 min, 81 ± 4% of the *P. aeruginosa*, was inactivated by the chitosan/CA(5.0%)/PEO nanofiber mats. This work is the first demonstration that an essential oil can be incorporated into and successfully delivered from nanofiber mats. The release of CA from the chitosan/PEO nanofiber mats offers potential as a flexible scaffold that can alleviate nosocomial infections by delivering a broad-spectrum natural antimicrobial agent.

Acknowledgements

This work was partially supported by an NSF-BRIGE grant (EEC-1342343), the James M. Douglas Career Development Faculty Award, and the NSF-sponsored ICE IGERT program (DGE-0654128). Thanks to Luke Williams and Dr. Paul J. Dauenhauer for assistance with GC, Nathaniel Eagan for assistance with lab work, and Jan Panteli for help with bacteria culture. Thanks to Drs. David A. Reckhow and Neil St. John Forbes for kindly allowing us use of their UV–vis and fluorescence microscope, respectively. Thanks to Dr. Weiguo Hu for guidance with NMR, as well as Dr. Alexander Ribbe and Lou Raboin for guidance with SEM. We acknowledge the use of facilities at the W.M. Keck Center for Electron Microscopy and the MRSEC at UMass Amherst.

References

An, J., Zhang, H., Zhang, J., Zhao, Y., & Yuan, X. (2009). Preparation and antibacterial activity of electrospun chitosan/poly(ethylene oxide) membranes containing silver nanoparticles. *Colloid and Polymer Science*, *287*, 1425–1434.
Angeles, M., Cheng, H., & Velankar, S. S. (2008). Emulsion electrospinning: Composite fibers from drop breakup during electrospinning. *Polymers for Advanced Technologies*, *19*, 728–733.
Aranaz, I., Mengibar, M., Harris, R., Panos, I., Miralles, B., Acosta, N., Galed, G., & Heras, A. (2009). Functional characterization of chitin and chitosan. *Current Chemical Biology*, *3*, 203–230.
(2004). *ASTM E2149-01. Standard test method for determining the antimicrobial activity of immobilized antimicrobial agents under dynamic contact conditions*. American Society for Testing and Materials.
Badawy, M. E. I., & Rabea, E. I. (2011). A biopolymer chitosan and its derivatives as promising antimicrobial agents against plant pathogens and their applications in crop protection. *International Journal of Carbohydrate Chemistry*, 1–29.
Badawy, M. E. I., & Rabea, E. I. (2013). Synthesis and structure–activity relationship of *N*-(cinnamyl) chitosan analogs as antimicrobial agents. *International Journal of Biological Macromolecules*, *57*, 185–192.
Bakkali, F., Averbeck, S., Averbeck, D., & Idaomar, M. (2008). Biological effects of essential oils–A review. *Food and Chemical Toxicology*, *46*, 446–475.
Briggs, T., & Arinzeh, T. L. (2014). Examining the formulation of emulsion electrospinning for improving the release of bioactive proteins from electrospun fibers. *Journal of Biomedical Materials Research A*, *102*, 674–684.
Burt, S. (2004). Essential oils: Their antibacterial properties and potential applications in foods–A review. *International Journal of Food Microbiology*, *94*, 223–253.
Chen, L., Bromberg, L., Hatton, T. A., & Rutledge, G. C. (2008). Electrospun cellulose acetate fibers containing chlorhexidine as a bactericide. *Polymer*, *49*, 1266–1275.
Cordes, E. H., & Jencks, W. P. (1962). On the mechanism of Schiff base formation and hydrolysis. *Journal of American Chemical Society*, *84*, 832–837.
Cserháti, T., Forgács, E., & Oros, G. (2002). Biological activity and environmental impact of anionic surfactants. *Environment International*, *28*, 337–348.
De Kievit, T. R. (2009). Quorum sensing in *Pseudomonas aeruginosa* biofilms. *Microbiology*, *11*, 279–288.
Donlan, R. M. (2002). Biofilms: Microbial life on surfaces. *Emerging Infectious Diseases*, *8*, 881–890.
Dorman, H. J., & Deans, S. G. (2000). Antimicrobial agents from plants: Antibacterial activity of plant volatile oils. *Journal of Applied Microbiology*, *88*, 308–316.
Edris, A. E. (2007). Pharmaceutical and therapeutic potentials of essential oils and their individual volatile constituents: A review. *Phytotherapy Research*, *21*, 308–323.
Engel, Y., Schiffman, J. D., Goddard, J. M., & Rotello, V. M. (2012). Nanomanufacturing of biomaterials. *Materials Today*, *15*, 478–485.
Fernandez-Megia, E., Novoa-Carballal, R., Quiñoá, E., & Riguera, R. (2005). Optimal routine conditions for the determination of the degree of acetylation of chitosan by ^{1}H-NMR. *Carohydrate Polymers*, *61*, 155–161.
Fick, R. B., Jr. (Ed.). (1993). *Pseudomonas aeruginosa*. The microbial hyena and its role in disease. In *Pseudomonas aeruginosa, the opportunist, pathogensis and disease*.
Frey, M. W. (2008). Electrospinning cellulose and cellulose derivatives. *Polymer Reviews*, *48*, 378–391.
Friedman, M., Kozukue, N., & Harden, L. A. (2000). Cinnamaldehyde content in foods determined by gas chromatography–mass spectrometry. *Journal of Agricultural and Food Chemistry*, *48*, 5702–5709.
Fu, J., Ji, J., Yuan, W., & Shen, J. (2005). Construction of anti-adhesive and antibacterial multilayer films via layer-by-layer assembly of heparin and chitosan. *Biomaterials*, *26*, 6684–6692.
Ganjian, I., Baumgarten, R. L., & Valenzuela, R. J. (1992). Using spin-spin decoupling NMR for structure elucidation in the extraction of cinnamaldehyde. *Journal of Chemical Education*, *69*, 511.
Guinesi, L. S., & Cavalheiro, É. T. G. (2006a). Influence of some reactional parameters on the substitution degree of biopolymeric Schiff bases prepared from chitosan and salicylaldehyde. *Carbohydrate Polymers*, *65*, 557–561.
Guinesi, L. S., & Cavalheiro, É. T. G. (2006b). The use of DSC curves to determine the acetylation degree of chitin/chitosan samples. *Thermochimica Acta*, *444*, 128–133.

Hammer, K. A., Carson, C. F., & Riley, T. V. (1999). Antimicrobial activity of essential oils and other plant extracts. *Journal of Applied Microbiology*, *86*, 985–990.
Helander, I. M., Nurmiaho-Lassila, E. L., Ahvenainen, R., Rhoades, J., & Roller, S. (2001). Chitosan disrupts the barrier properties of the outer membrane of gram-negative bacteria. *International Journal of Food Microbiology*, *71*, 235–244.
Hirai, A., Odani, H., & Nakajima, A. (1991). Determination of degree of deacetylation of chitosan by ^{1}H NMR spectroscopy. *Polymer Bulletin*, *26*, 87–94.
Honarkar, H., & Barikani, M. (2009). Applications of biopolymers. I: Chitosan. *Chemical Monthly*, *140*, 1403–1420.
Iamsamai, C., Hannongbua, S., Ruktanonchai, U., Soottitantawat, A., & Dubas, S. T. (2010). The effect of the degree of deacetylation of chitosan on its dispersion of carbon nanotubes. *Carbon*, *48*, 25–30.
Jatunov, S., Franconetti, A., Gomez-Guillen, M., & Cabrera-Escribano, F. (2012). Design of aromatic aldehyde chitosan derivatives for biological and industrial applications. *Sciforum Electronic Conference Series*, *16*.
Jia, P., Xue, Y. J., Duan, X. J., & Shao, S. H. (2011). Effect of cinnamaldehyde on biofilm formation and sarA expression by methicillin-resistant *Staphylococcus aureus*. *Letters in Applied Microiology*, *53*, 409–416.
Kavanaugh, N. L., & Ribbeck, K. (2012). Selected antimicrobial essential oils eradicate *Pseudomonas* spp. and *Staphylococcus aureus* biofilms. *Applied and Environmental Microbiology*, *78*, 4057–4061.
Kleven, R., Edwards, J., Richards, C., & Horan, T. (2007). Estimating health care-associated infections and deaths in U.S. hospitals, 2002. *Public Health Reports*, *122*, 160–166.
Krajewska, B. (2005). Membrane-based processes performed with use of chitin/chitosan materials. *Separation and Purification Technology*, *41*, 305–312.
Krajewska, B., Wydro, P., & Jańczyk, A. (2011). Probing the modes of antibacterial activity of chitosan, effects of pH and molecular weight on chitosan interactions with membrane lipids in Langmuir films. *Biomacromolecules*, *12*, 4144–4152.
Krajewska, B., Kyzioł, A., & Wydro, P. (2013a). Chitosan as a subphase disturbant of membrane lipid monolayers. The effect of temperature at varying pH: II. DPPC and cholesterol. *Colloids and Surfaces A: Physicochemical and Engineering Aspects*, *434*, 359–364.
Krajewska, B., Wydro, P., & Kyzioł, A. (2013b). Chitosan as a subphase disturbant of membrane lipid monolayers. The effect of temperature at varying pH: I. DPPG. *Colloids and Surfaces A: Physicochemical and Engineering Aspects*, *434*, 349–358.
Li, Y., Ko, F. K., & Hamad, W. Y. (2013). Effects of emulsion droplet size on the structure of electrospun ultrafine biocomposite fibers with cellulose nanocrystals. *Biomacromolecules*, *14*, 3801–3807.
Liu, H., Du, Y., Wang, X., & Sun, L. (2004). Chitosan kills bacteria through cell membrane damage. *International Journal of Food Microbiology*, *95*, 147–155.
Liu, S.-J., Kau, Y.-C., Chou, C.-Y., Chen, J.-H., Wu, R.-C., & Yeh, W.-L. (2010). Electrospun PLGA/collagen nanofibrous membrane as early-stage wound dressing. *Journal of Membrane Science*, *355*, 53–59.
López, P., Sanchez, C., Batlle, R., & Nerín, C. (2007). Vapor-phase activities of cinnamon, thyme, and oregano essential oils and key constituents against foodborne microorganisms. *Journal of Agricultural and Food Chemistry*, *55*, 4348–4356.
Muzzarelli, R. A. A. (1977). *Chitin*. Oxford: Pergamon Press Ltd.
Muzzarelli, R. A. A. (2012). Nanochitins and nanochitosans, paving the way to eco-friendly and energy-saving exploitation of marine resources, Polymer Science: A comprehensive reference. *Polymer Science: A Comprehensive Reference*, *10*, 153–164.
Muzzarelli, R. A. A., Boudrant, J., Meyer, D., Manno, N., DeMarchis, M., & Paoletti, M. G. (2012). A tribute to Henri Braconnot, precursor of the carbohydrate polymers science, on the chitin bicentennial. *Carbohydrate Polymers*, *87*, 995–1012.
Niu, C., Afre, S., & Gilbert, E. S. (2006). Subinhibitory concentrations of cinnamaldehyde interfere with quorum sensing. *Letters in Applied Microbiology*, *43*, 489–494.
Ojagh, S. M., Rezaei, M., Razavi, S. H., & Hosseini, S. M. H. (2010). Development and evaluation of a novel biodegradable film made from chitosan and cinnamon essential oil with low affinity toward water. *Food Chemistry*, *122*, 161–166.
Ooi, L. S. M., Li, Y., Kam, S.-L., Wang, H., Wong, E. Y. L., & Ooi, V. E. C. (2006). Antimicrobial activities of cinnamon oil and cinnamaldehyde from the Chinese medicinal herb *Cinnamomum cassia* blume. *The American Journal of Chinese Medicine*, *34*, 511–522.
Oussalah, M., Caillet, S., & Lacroix, M. (2006). Mechanism of action of Spanish oregano, Chinese cinnamon, and savory essential oils against cell membranes and walls of *Escherichia coli* O157:H7 and *Listeria monocytogenes*. *Journal of Food Protection*, *69*, 1046–1055.
Page, M. G. P., & Heim, J. (2009). Prospects for the next anti-Pseudomonas drug. *Current Opinion in Phamacology*, *9*, 558–565.
Pakravan, M., Heuzey, M.-C., & Ajji, A. (2011). A fundamental study of chitosan/PEO electrospinning. *Polymer*, *52*, 4813–4824.
Pattnaik, S., Suramanyam, V. R., Bapaji, M., & Kole, C. R. (1997). Antibacterial and antifungal activity of aromatic constituents of essential oils. *Microbiology*, *89*, 39–46.
Peppas, N. A., Bures, P., Leobandung, W., & Ichikawa, H. (2000). Hydrogels in pharmaceutical formulations. *European Journal of Pharmaceutics and Biopharmaceutics*, *50*, 27–46.
Pine, S. H., Hendrickson, J., Cram, D. J., & Hammono, G. S. (1980). *Organic Chemistry* (4th ed., pp. 285–286). New York, NY: McGrawHill.
Rabea, E. I., Badawy, M. E.-T., Stevens, C. V., Smagghe, G., & Steurbaut, W. (2003). Chitosan as antimicrobial agent: Applications and mode of action. *Biomacromolecules*, *4*, 1457–1465.
Rasmussen, T. B., & Givskov, M. (2006). Quorum-sensing inhibitors as anti-pathogenic drugs. *Medical Microbiology*, *296*, 149–161.
Rieger, K. A., Birch, N. P., & Schiffman, J. D. (2013). Designing electrospun nanofiber mats to promote wound healing—A review. *Journal of Materials Chemistry B*, *36*, 4531–4541.
Rinaudo, M. (2006). Chitin and chitosan: Properties and applications. *Progress in Polymer Science*, *31*, 603–632.
Rodraguez, M. (2002). Emulsification capacity of chitosan. *Carbohydrate Polymers*, *48*, 271–276.
Rutledge, G. C., & Fridrikh, S. V. (2007). Formation of fibers by electrospinning. *Advanced Drug Delivery Reviews*, *59*, 1384–1391.
Sanders, E. H., Kloefkorn, R., Bowlin, G. L., Simpson, D. G., & Wnek, G. E. (2003). Two-phase electrospinning from a single electrified jet: Microencapsulation of aqueous reservoirs in poly(ethylene-*co*-vinyl acetate) fibers. *Macromolecules*, *36*, 3803–3805.
Schiffman, J. D., & Schauer, C. L. (2007a). Cross-linking chitosan nanofibers. *Biomacromolecules*, *8*, 594–601.
Schiffman, J. D., & Schauer, C. L. (2007b). One-step electrospinning of cross-linked chitosan fibers. *Biomacromolecules*, *8*, 2665–2667.
Schiffman, J. D., & Schauer, C. L. (2008). A review: Electrospinning of biopolymer nanofibers and their applications. *Polymer Reviews*, *48*, 317–352.
Schiffman, J. D., Wang, Y., Giannelis, E. P., & Elimelech, M. (2011). Biocidal activity of plasma modified electrospun polysulfone mats functionalized with polyethyleneimine-capped silver nanoparticles. *Langmuir*, *27*, 13159–13164.
Schulz, P. C., Rodríguez, M. S., Del Blanco, L. F., Pistonesi, M., & Agulló, E. (1998). Emulsification properties of chitosan. *Colloid and Polymer Science*, *276*, 1159–1165.
Siepmann, J., & Peppas, N. A. (2011). Higuchi equation: Derivation, applications, use and misuse. *International Journal of Pharmaceutics*, *418*, 6–12.
Talrose, V., Yermakov, A. N., Usov, A. A., Goncharova, A. A., Leskin, A., Messineva, N. A., & Efimkina, M. V. (2007). UV/visible spectrum. In P. J. Linstrom, & W. G. Mallard (Eds.), *NIST chemistry WebBook. NIST standard reference database number 69*. Gaithersburg: National Institute of Standards and Technology.
Teo, W. E., & Ramakrishna, S. (2006). A review on electrospinning design and nanofibre assemblies. *Nanotechnology*, *17*, R89–R106.
Varum, K. M., Antohonsen, M. W., Grasdalen, H., & Smidsrød, O. (1991). Determination of the degree of *N*-acetylation and the distribution of nacetyl groups in partially *N*-deacetylated chitins (chitosans) by high-field NMR spectroscopy. *Carbohydrate Research*, *211*, 17–23.
Verreck, G., Chun, I., Rosenblatt, J., Dijck, A. V. J., Noppe, M., & Brewster, M. M. E. (2003). Incorporation of drugs in an amorphous state into electrospun nanofibers composed of a water-insoluble, nonbiodegradable polymer. *Journal of Control Release*, *92*, 349–360.
Xu, X., Yang, L., Xu, X., Wang, X., Chen, X., Liang, Q., Zeng, J., & Jing, X. (2005). Ultrafine medicated fibers electrospun from W/O emulsions. *Journal of Controlled Release*, *108*, 33–42.
Xu, X., Zhuang, X., Chen, X., Wang, X., Yang, L., & Jing, X. (2006). Preparation of core–sheath composite nanofibers by emulsion electrospinning. *Macromolecular Rapid Communications*, *27*, 1637–1642.
Yan, L. Y., Poon, Y. F., Chan-Park, M. B., Chen, Y., & Zhang, Q. (2008). Individually dispersing single-walled carbon nanotubes with novel neutral pH water-soluble chitosan derivatives. *The Journal of Physical Chemistry C*, *112*, 7579–7587.
Yang, J., Kuang, X., Li, B., Zhou, B., Li, J. B., & Cui, M. A. M. (2012). Study on release mechanism of inhibitory components from cinnamon and clove powders. *Journal of Food Safety*, *32*, 189–197.
Zhang, Y., Lim, C. T., Ramakrishna, S., & Huang, Z.-M. (2005). Recent development of polymer nanofibers for biomedical and biotechnological applications. *Journal of Materials Science: Materials in Medicine*, *16*, 933–946.
Zodrow, K. R., Schiffman, J. D., & Elimelech, M. (2012). Biodegradable polymer (PLGA) coatings featuring cinnamaldehyde and carvacrol mitigate biofilm formation. *Langmuir*, *39*, 13993–13999.